

# On Safer Reinforcement Learning Policies for Sedation and Analgesia in Intensive Care

Joel Romero-Hernández

*BCN MedTech, Complex Systems Lab  
Universitat Pompeu Fabra  
Barcelona, Spain  
joel.romero@upf.edu*

Oscar Camara

*BCN MedTech, PhySense Group  
Universitat Pompeu Fabra  
Barcelona, Spain  
oscar.camara@upf.edu*

**Abstract**—Pain management in intensive care usually involves complex trade-offs between therapeutic goals and patient safety, since both inadequate and excessive treatment may induce serious sequelae. Reinforcement learning can help address this challenge by learning medication dosing policies from retrospective data. However, prior work on sedation and analgesia has optimized for objectives that do not value patient survival while relying on algorithms unsuitable for imperfect information settings. We investigated the risks of these design choices by implementing a deep reinforcement learning framework to suggest hourly medication doses under partial observability. Using data from 47,144 ICU stays in the MIMIC-IV database, we trained policies to prescribe opioids, propofol, benzodiazepines, and dexmedetomidine according to two goals: reduce pain or jointly reduce pain and mortality. We found that, although the two policies were associated with lower pain, actions from the first policy were positively correlated with mortality, while those proposed by the second policy were negatively correlated. This suggests that valuing long-term outcomes could be critical for safer treatment policies, even if a short-term goal remains the primary objective.

**Index Terms**—Reinforcement Learning, AI Safety, Intensive Care, Pain Management

## I. INTRODUCTION

Critically ill patients often experience pain, which can disrupt cardiorespiratory function, lead to emotional distress, and induce long-term sequelae [1]. Despite the availability of several analgesic and sedative medications, their use can also have profound, even life-threatening effects [2], [3]. Thus, pain management requires striking a delicate balance between effective pain relief and patient stability [4].

This is particularly challenging in the intensive care unit (ICU), where patients often have comorbidities that increase vulnerability to side effects [5]–[7]. Indeed, there are indications that nearly 70% of patients suffer from unrecognized or undertreated pain [8], which increases the likelihood of developing chronic pain after ICU discharge. Over 100 million Americans suffered from chronic pain in 2010, resulting in an economic loss ranging from \$560 to \$635 billion, higher than that for heart diseases or cancer [9], [10].

Offline reinforcement learning (RL) can help clinicians address this task by identifying optimal dosing policies from retrospective data [11]. Unlike traditional RL, this avoids the ethical concerns of trial-and-error learning on actual patients.

In sedation and analgesia, data-driven RL has been previously explored, albeit using limited datasets, low-dimensional action spaces, and without accounting for mortality or partial observability [12], both inherent to the ICU.

We hypothesize that these design choices may yield policies that put patients at risk in exchange for modest short-term gains. Not penalizing mortality, for instance, could create perverse incentives to prioritize actions associated with death after discharge if these are correlated with lower reported pain during the ICU stay. In turn, this behavior could be accentuated by the rigidity of simple action spaces and the absence of strategies to manage imperfect information in sequential decision-making.

As illustrated in Fig. 1, our work addresses these questions through three main contributions. First, we defined reward functions that value both pain relief and survival up to 30 days after discharge. Second, we approached partial observability and learning without exploration by combining offline RL with recurrent representations of the patient state. Third, we learned policies with continuous, real-valued action spaces on a more extensive and diverse dataset.

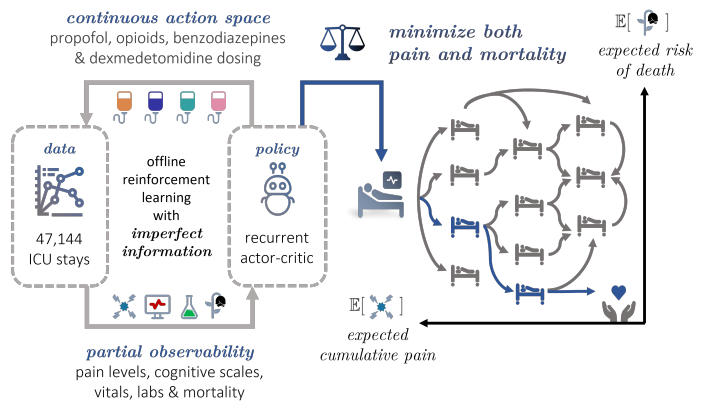


Fig. 1. Schematic of our data-driven reinforcement learning (RL) framework for sedation and analgesia in the intensive care unit (ICU). We used offline RL with partial observability to train, validate, and test recurrent agents on 47,144 ICU stays. Specifically, we trained policies to recommend propofol, opioids, benzodiazepines, and dexmedetomidine doses per hour, seeking to minimize pain and mortality. The agents operated based on observations, including vital signs, pain reports, and laboratory values. We studied their behavior to elucidate which objectives encouraged safer strategies.

## II. RELATED WORK

Data-driven RL has been explored in the ICU not only for sedation and analgesia, but also for heparin, vasopressor, fluid, insulin, or oxygen therapies [13]–[17]. These approaches rely on electronic health records (EHRs), which are converted into multivariate time series. Usually, RL agents are trained off-policy to prescribe medications that maximize the reward function, while held-out trajectories are used for offline evaluation.

Prasad et al. [18] investigated the optimization of sedation and mechanical ventilation using records of 2,464 successfully discharged patients from MIMIC-III. Fitted Q-iteration (FQI) agents were trained to choose among four sedative doses, using a reward function that valued both vital sign stability and ventilation performance. Similarly, Yu et al. [19], [20] worked with a subset of 707 cases and used that reward structure to train agents that imitated the clinician policy.

Lopez-Martinez et al. [21] introduced pain as an observation and proposed dueling double deep Q networks that selected morphine doses from 14 options. This work leveraged a larger dataset by curating records from 6,843 stays in MIMIC-III and employed a reward function that valued pain reduction, heart rate, and respiratory rate stability.

Eghbali et al. [22], [23] focused on sedation with two continuous actions: a sedative (propofol) and an opioid analgesic (fentanyl). The authors extracted records from 1,757 adult patients in MIMIC-IV, and a deep deterministic policy gradient agent was trained to optimize mean arterial pressure. They also explored a discrete action space with 27 options: 9 doses for propofol, fentanyl, and midazolam.

In summary, previous studies considered at most 6,843 ICU stays, represented as sequences of hourly observations that could include vital signs, ventilation status, sedation, pain levels, medication dosages, and demographics. Only one study explored two continuous actions, while most assumed discretized interventions (with up to 27 options). Some works utilized methods suitable for learning without exploration, such as FQI, yet none explicitly incorporated survival as a constraint or optimization objective, nor modeled the effect of past observations on the patient’s current state.

Building on this prior work, we investigated the effects of penalizing mortality, modeling patient state using recurrent representations, optimizing over four continuous actions, and learning from a larger dataset comprising 47,144 ICU stays.

## III. BACKGROUND

**RL.** Sequential decision problems can be modeled as a Markov decision process (MDP)  $(\mathcal{S}, \mathcal{A}, p, r, \gamma)$  with state space  $\mathcal{S}$ , action space  $\mathcal{A}$ , and a state transition function  $p(\mathbf{s}_{t+1}|\mathbf{s}_t, \mathbf{a}_t)$  that follows the Markov property. The reward function  $r$  assigns a scalar  $r_t$  to each state-action tuple, and the discount factor  $\gamma \in [0, 1)$  ensures a bounded cumulative reward, the return  $G_t = \sum_{k=0}^{\infty} \gamma^k r_{t+k}$ . The objective is to learn a policy  $\pi$  that maximizes the expected return  $J(\pi) = \mathbb{E}_{\pi}[G_t]$ , i.e., an optimal policy  $\pi^* = \text{argmax}_{\pi} J(\pi)$ . This is often achieved by optimizing action values  $q(\mathbf{s}_t, \mathbf{a}_t) = \mathbb{E}[G_t|\mathbf{s}_t, \mathbf{a}_t]$ , such that  $q^*(\mathbf{s}_t, \mathbf{a}_t) = \max_{\pi} q_{\pi}(\mathbf{s}_t, \mathbf{a}_t)$  [24].

**Deep RL.** Neural networks can be combined with RL to learn deterministic continuous control policies. This may be done by training a value network  $Q_{\theta}$  and a policy network  $\pi_{\phi}$ , where  $\theta$  and  $\phi$  are their parameters [25]. Here,  $Q_{\theta}$  learns to estimate  $q_{\pi_{\phi}}(\mathbf{s}_t, \mathbf{a}_t)$  by minimizing the Bellman error between the value predicted for  $\pi_{\phi}$ ’s actions and the Bellman targets  $y_t = r_t + \gamma Q_{\theta'}(\mathbf{s}_{t+1}, \pi_{\phi'}(\mathbf{s}_{t+1}))$ . Concomitantly,  $\pi_{\phi}$  is trained to maximize  $J(\phi) = \mathbb{E}[Q_{\theta}(\mathbf{s}_t, \pi_{\phi}(\mathbf{s}_t))]$ . Here,  $Q_{\theta'}$  and  $\pi_{\phi'}$  are target networks, slowly-updated to stabilize learning [26].

**Offline learning.** Training  $Q_{\theta}$  from experiences collected by an arbitrary policy involves an important extrapolation error: incomplete coverage of the state-action space leads to biased value estimates and underperforming policies [27], something compounded by function approximation [28], [29]. Offline RL introduces strategies to minimize the distributional shift between the target and behavior policy, decreasing the influence of these out-of-distribution actions [30], [31].

**Partial observability.** A partially observable Markov decision process (POMDP)  $(\mathcal{S}, \mathcal{A}, \mathcal{O}, p, e, r, \gamma)$  models imperfect information as a space of observations  $\mathcal{O}$  [32]. In a POMDP, the emission function  $e$  maps each hidden state  $\mathbf{s}_t$  to an observation  $\mathbf{o}_t \in \mathcal{O}$ . Because  $\mathbf{s}_{t+1}$  depends on  $\mathbf{s}_t$ , observations do not satisfy the Markov property. Instead, a sufficient statistic can be constructed from the current history of observations and actions,  $\mathbf{h}_t = (\mathbf{o}_0, \mathbf{a}_0, \mathbf{o}_1, \mathbf{a}_1, \dots, \mathbf{o}_{t-1}, \mathbf{a}_{t-1}, \mathbf{o}_t)$ .

## IV. METHODS

### A. Formalization

**Model.** We formulated pain management as a POMDP where  $\mathbf{s}_t \in \mathcal{S} \subseteq \mathbb{R}^{d_s}$  is the hidden,  $d_s$ -dimensional state of the patient,  $\mathbf{a}_t \in \mathcal{A} \subseteq \mathbb{R}^{d_a}$  is a vector of doses administered for  $d_a$  medications of interest, and  $\mathbf{o}_t \in \mathcal{O} \subseteq \mathbb{R}^{d_o}$  is a vector of  $d_o$  observations taken from the patient. The state transition function  $p$  captures the unknown mechanics of the patient system, and the emission function  $e$  represents the processes mapping these latent dynamics to measurements. Finally, the reward function  $r$  and the discount factor  $\gamma$  encode the objectives and priorities for some dosing policy  $\pi$ .

**Trajectories.** A trajectory  $\tau^i$  describes the evolution of an ICU stay  $i$  according to the POMDP. It includes a sequence of  $T_i$  observation-action tuples  $(\mathbf{o}_t^i, \mathbf{a}_t^i)$ , and a binary outcome  $m^i$ , with  $m^i = 0$  if the patient survived and  $m^i = 1$  if the patient died. Every measurement  $\mathbf{o}_t^i$  contains a dimension  $s_t^i \in \{0, 1, \dots, s_{\max}\}$  encoding the patient’s reported pain for time step  $t$ . Hence, each trajectory is defined as a tuple  $\tau^i = ((\mathbf{o}_t^i, \mathbf{a}_t^i)_{t=0}^{T_i-1}, m^i)$  with a reward sequence  $(r_t^i)_{t=0}^{T_i-1}$ , where  $r_{T_i-1}^i$  can include an additional terminal reward.

**Policy.** We define the reward function  $r$  to score the utility of sedative and analgesic dosing decisions. We aim to learn policies  $\pi$  that maximize  $\mathbb{E}[G_t]$  from a dataset  $\mathcal{D}$  containing  $N$  pre-recorded trajectories. To approximate a sufficient statistic for decision-making under partial observability, we define pain management policies as maps  $\pi : \mathcal{H} \rightarrow \mathcal{A}$  from history vectors  $\mathbf{h}_t^i \in \mathcal{H}$  to action vectors  $\mathbf{a}_t^i$ . Here,  $\mathcal{H}$  is the space of possible histories and  $\mathbf{a}_t^i$  encodes the  $d_a$  doses administered to the patient at time step  $t$  for trajectory  $i$ .

**Reward functions.** Our reward structure incorporates two weighted terms. As shown in (1), the first term penalizes higher levels of pain per time step, normalized by stay length and scaled by weight  $w_s$ . The second term, scaled by weight  $w_m$ , introduces an explicit terminal penalty for mortality, which is added to the reward at the last time step.

$$r_t^i = -w_s \cdot \frac{\zeta_t^i}{T_i \cdot \zeta_{\max}} - w_m \cdot \mathbb{I}_{\{t=T_i-1\}} \cdot m^i \quad (1)$$

Thus, the relative importance of the two sub-goals for a given policy can be determined by simply adjusting the  $w_m/w_s$  ratio.

### B. Data engineering

As represented in Fig. 2, the MIMIC-IV database [33] was utilized to curate a dataset with 47,144 stays from 30,087 adult patients. Each stay trajectory was encoded as a 22-dimensional hourly time series, comprising both quantitative (e.g., blood pressure, heart rate) and ordinal (e.g., reported pain intensity) features, as well as a binary survival marker.

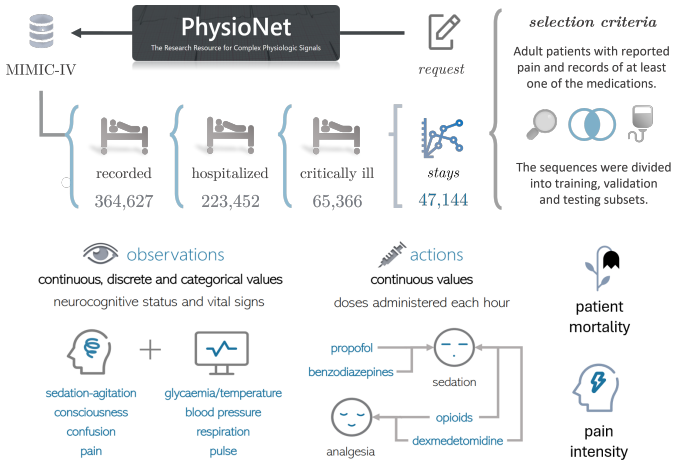


Fig. 2. Our dataset included both quantitative and ordinal observations, apart from four continuous medication actions per hour.

**Observations.** The observation space  $\mathcal{O}$  included vital signs (heart rate, respiratory rate, pulse oxygen saturation, mean, systolic, and diastolic blood pressure), body temperature, urine output, laboratory values (glucose, potassium, sodium, chloride, bicarbonate, creatinine, and blood urea nitrogen), and cognitive assessment scales (pain intensity, Glasgow coma scores, sedation-agitation, and delirium).

**Actions.** The action space  $\mathcal{A}$  incorporated four continuous dimensions populated with dosing records from eight sedatives and analgesics. Firstly, we expressed opioid administrations as a combined dose per hour by converting fentanyl and hydro-morphone doses into oral morphine-equivalent mg [34] and merging these with pre-existing morphine records. Secondly, we normalized propofol doses into mg per kg [35]. Thirdly, we reported benzodiazepine doses as midazolam-equivalent mg by converting diazepam records into lorazepam-equivalent mg [36], merging these with lorazepam doses, and then converting to midazolam-equivalent mg [37]. Lastly, dexmedetomidine doses were normalized in mg per kg [38].

**Outlier removal.** Following the approach in prior preprocessing pipelines, quantile-based data cleaning was applied to continuous variables [39]. For vital signs, values below the 0.05th percentile and above the 99.95th percentile were deleted. For laboratory values, the thresholds were 0.1th and 99.9th. For urine output and medication doses, values beyond the 99.9th percentile and the 99th percentile were deleted.

**Imputation.** To fill missing values, we first applied a basic sample-and-hold method (last observation carried forward) according to feature-specific clinical thresholds [40]. Then, we implemented a pipeline based on multiple imputation by chained equations (MICE) to iteratively estimate the remaining missing values [41]. We chose gradient boosting machines (GBMs) with decision trees (DTs) [42] as our predictive model for two main reasons. On the one hand, DTs are well-suited for capturing intricate non-linear relationships among both quantitative and categorical variables [43]. On the other hand, DT ensembles have been reported to achieve state-of-the-art performance in various complex tasks [44], [45].

### C. Architecture and algorithm

To learn our policies, we implemented an architecture with three distinct modules. First, a recurrent neural network with gated recurrent units [46] and parameters  $\psi$ ,  $\text{GRU}_\psi$ . Second, two critic networks  $Q_{\theta_1}$  and  $Q_{\theta_2}$ , with target networks  $Q_{\theta'_1}$  and  $Q_{\theta'_2}$ . Third, an actor network  $\pi_\phi$  with target network  $\pi_{\phi'}$ . Fig. 3 shows an overview of how the modules interact, while the text below details the loss functions we minimized.

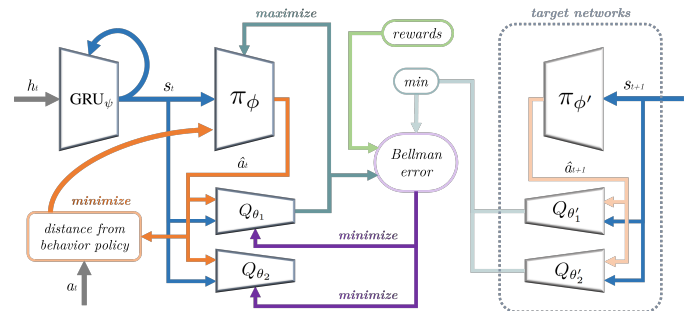


Fig. 3. Our actor-critic architecture addresses both imperfect information and offline learning. The recurrent representation network  $\text{GRU}_\psi$  learns to capture the influence of past observations, thereby approximating the patient state. Subsequently, the behavior-regularized actor  $\pi_\phi$  proposes actions based on those states, which are evaluated by the critics  $Q_{\theta_1}$  and  $Q_{\theta_2}$ .

**State representation.**  $\text{GRU}_\psi$  was trained to approximate a  $\mathcal{H} \rightarrow \mathcal{S}$  map by learning compact representations from histories of observations and actions [47]. As shown in (2), this was done in a supervised manner, focusing on predicting both future observation vectors  $\mathbf{o}_{t+1}^i$  and mortality  $m^i$ , where  $m_t^i$  is the death probability predicted at time  $t$ .

$$\mathcal{L}_{\text{GRU}}(\psi) = \|\mathbf{o}_{t+1}^i - \hat{\mathbf{o}}_{t+1}^i\|_2^2 + 0.2 \cdot \ell_m(m^i, \hat{m}_t^i) \quad (2)$$

$$\ell_m(m^i, \hat{m}_t^i) = -m^i \log(\hat{m}_t^i) - (1 - m^i) \log(1 - \hat{m}_t^i) \quad (3)$$

The mortality prediction term (3) was down-scaled by 0.2 to encourage the learning of representations that could capture both relevant short-term dynamics and long-term outcomes.

**Double critic.** On top of those representations, we trained  $Q_{\theta_1}$  and  $Q_{\theta_2}$  to independently estimate expected cumulative rewards for continuous medication doses: that is, to approximate maps  $\mathcal{S} \times \mathcal{A} \rightarrow \mathbb{R}$  by estimating the expected return  $G_t$  given a specific reward function  $r$ . Each of the critics consisted of a multi-layer perceptron (MLP) trained to minimize the mean squared error between its value estimates and Bellman targets. As shown in Fig. 3, this was computed using the lowest prediction among both networks.

$$y_t^i = r_t^i + \gamma \min_{j=1,2} Q_{\theta_j}(\mathbf{s}_{t+1}^i, \pi_{\phi}(\mathbf{s}_{t+1}^i)) \quad (4)$$

This pessimistic value estimation process has been proven to mitigate the overestimation bias in value-based RL methods [48]. As suggested in previous research, Bellman targets were computed using slowly updated copies of the networks, which were regulated by the Polyak averaging coefficient  $\kappa$ .

$$\mathcal{L}_Q(\theta_j) = \mathbb{E}_{\mathcal{D}} \left[ (Q_{\theta_j}(\mathbf{s}_t^i, \mathbf{a}_t^i) - y_t^i)^2 \right] \quad j \in \{1, 2\} \quad (5)$$

**Behavior-regularized actor.** We trained  $\pi_{\phi}$  (also an MLP) to learn a mapping  $\mathcal{S} \rightarrow \mathcal{A}$  that maximized  $Q_{\theta_1}$  value estimates. Following prior work on minimalist offline RL [49], actor updates were regularized with a behavior cloning objective that penalized deviation from clinician actions.

$$\mathcal{L}_{\pi}(\phi) = \mathbb{E}_{\mathcal{D}} \left[ -\lambda Q_{\theta_1}(\mathbf{s}_t^i, \pi_{\phi}(\mathbf{s}_t^i)) + \|\pi_{\phi}(\mathbf{s}_t^i) - \mathbf{a}_t^i\|_2^2 \right] \quad (6)$$

This mitigates extrapolation error by constraining the actor to decisions empirically supported by the data distribution. Here,  $\lambda$  acts as an adaptive normalization for critic values that ensures scale consistency between both terms. In this context, the importance of value maximization relative to behavior cloning can be tuned by increasing the hyperparameter  $\alpha$ .

$$\lambda = \frac{\alpha}{\mathbb{E}_{\mathcal{D}}[|Q_{\theta_1}(\mathbf{s}_t^i, \mathbf{a}_t^i)|]} \quad (7)$$

#### D. Experiments

We learned two distinct policies. In both cases, we set  $w_{\varsigma} > 0$ .

- **Policy A.** We set  $w_m = 0$  to train a policy  $\pi_{\phi_A}$  that only optimized for pain minimization. This was intended to model a strategy prioritizing short-term effectiveness.

$$\phi_A \in \operatorname{argmin}_{\phi} \left\{ w_{\varsigma} \mathbb{E}_{\pi_{\phi}, \mathcal{D}} \left[ \sum_{t=0}^{T_i-1} \frac{\varsigma_t^i}{T_i \cdot \varsigma_{\max}} \right] \right\} \quad (8)$$

- **Policy B.** We enforced  $w_m = 10 \cdot w_{\varsigma}$  to train a policy  $\pi_{\phi_B}$  that jointly minimized reported pain and mortality up to 30 days after discharge. Since both terms in (9) are normalized to lie in  $[0, 1]$ , choosing  $w_m > w_{\varsigma}$  ensures that a full-unit increase in mortality incurs a larger penalty than any possible improvement in the pain term. Thus, this was our proposal to model a safety-aware strategy.

$$\phi_B \in \operatorname{argmin}_{\phi} \left\{ w_{\varsigma} \mathbb{E}_{\pi_{\phi}, \mathcal{D}} \left[ \sum_{t=0}^{T_i-1} \frac{\varsigma_t^i}{T_i \cdot \varsigma_{\max}} \right] + w_m \mathbb{E}_{\pi_{\phi}, \mathcal{D}} [m^i] \right\} \quad (9)$$

**Data splits.** 64% of the ICU stays were used to train our representations and offline RL policies, while 16% were left for internal validation and model selection. Conversely, 20% of the stays were excluded from the learning process and reserved for policy analysis. This split was performed ensuring that no patient had stays in multiple subsets.

**Hyperparameters.** We explored various possible architectures and configurations, including different latent dimensions, types of recurrent units, activation functions, weight initialization methods, learning rates, and optimizers, among others. Table I provides a detailed overview of the final settings used, which provided a more stable and smooth learning process.

TABLE I  
NEURAL NETWORK ARCHITECTURE AND HYPERPARAMETERS.

Component	State Encoder	Critic	Actor
Input dimensionality	$d_o + d_a$	$d_s + d_a$	$d_s$
Output dimensionality	$d_s$	1	$d_a$
Latent dimensions	64	64	64
Hidden layers	2	2	2
Activation function	tanh	LeakyReLU	LeakyReLU
Weight initialization	Orthogonal	Orthogonal	Orthogonal
Base architecture	GRU	MLP	MLP
$\alpha$	—	—	2.0
$\gamma$	—	0.99	—
$\kappa$	—	0.005	0.005
Optimizer	Adam	Adam	Adam
Learning rate	$1 \times 10^{-4}$	$1 \times 10^{-4}$	$1 \times 10^{-4}$
Gradient clipping	0.5 (norm)	0.5 (norm)	0.5 (norm)

#### E. Policy analysis

In the absence of a provably accurate counterfactual model, we grounded our evaluation in simple, interpretable associations and metrics, always with reference to the empirical evidence in the data distribution.

For each learned policy, we computed a clinician-agent agreement score  $C_i$  for every trajectory  $i$  in the test set.

$$C_i = 1 - \frac{1}{d_a \cdot T_i} \sum_{k=1}^{d_a} \sum_{t=0}^{T_i-1} \frac{|a_t^{i,k} - \pi_{\phi}(\text{GRU}_{\psi}(\mathbf{h}_t^i))^k|}{a_{\max}^k} \quad (10)$$

As defined in (10), the agreement score corresponds to one minus the normalized mean absolute distance between the recorded clinician doses and the proposed doses. Here,  $d_a$  is the number of pharmacological actions,  $a_t^{i,k}$  is the dose recorded for action  $k$  at time  $t$ , and  $a_{\max}^k$  refers to the maximum dose recorded for that action in the entire test set.

We used this score to elucidate the general similarity between policies A and B and the clinician policy. Then, we identified in which cases the deviations were the greatest. To get insights into these differences, we extracted pre-admission diagnostic data and identified the comorbidity profiles associated with the most salient behaviors.

Subsequently, we examined associations between clinician-agent agreement, mortality up to 30 days after discharge, and cumulative pain by estimating bootstrapped Spearman rank correlations (1,000 resamples) in test cases. This choice avoids assumptions of linearity or scale and provides a more robust basis for policy comparison.

This analysis aimed to assess how closely each policy aligned with clinical strategies associated with specific outcomes. In addition, we evaluated the contribution of individual actions to the overall correlation. We also estimated bootstrapped correlations between patient comorbidity scores and deviation from doses prescribed by the clinicians.

## V. RESULTS

Policy A ( $\pi_{\phi_A}$ ) and policy B ( $\pi_{\phi_B}$ ) exhibited high average agreement with the doses recorded in test cases (Fig. 4). This observation is consistent with the behavior cloning objective playing a dominant role in the training process: both actors learned a strategy that statistically imitated the clinician's response in the most typical scenarios.

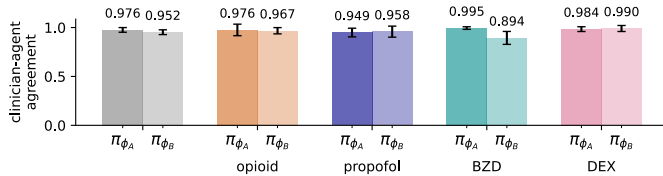


Fig. 4. Clinician-agent agreement for policies A ( $\pi_{\phi_A}$ ) and B ( $\pi_{\phi_B}$ ) in the test set. Bars show the mean similarity, overall and medication-specific, including opioids, propofol, benzodiazepines (BZD), and dexmedetomidine (DEX). Error bars indicate the standard deviation across patient stays.

Nevertheless, when examining the association between clinician-agent agreement, mortality, and cumulative pain, we observed marked differences between the two policies.

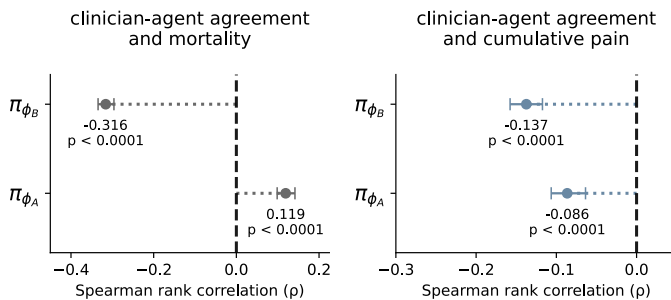


Fig. 5. Correlation between clinician-agent agreement and mortality (left) or cumulative pain (right) for policy A ( $\pi_{\phi_A}$ ) and policy B ( $\pi_{\phi_B}$ ). Points indicate correlation estimates, and horizontal bars represent confidence intervals. The vertical dashed line denotes no association ( $\rho = 0$ ).

As shown in Fig. 5, higher clinician-agent agreement with  $\pi_{\phi_A}$  was significantly associated with lower reported cumulative pain, but also with higher mortality up to 30 days after discharge. In contrast, agreement with  $\pi_{\phi_B}$  was significantly and negatively correlated with mortality, while also exhibiting a more pronounced negative correlation with cumulative pain.

This pattern is studied in greater detail in Fig. 6. Despite generally broad support for the action distribution proposed by  $\pi_{\phi_B}$ , increasing clinician-agent agreement was associated with both progressively lower empirical mortality rates and cumulative reported pain.

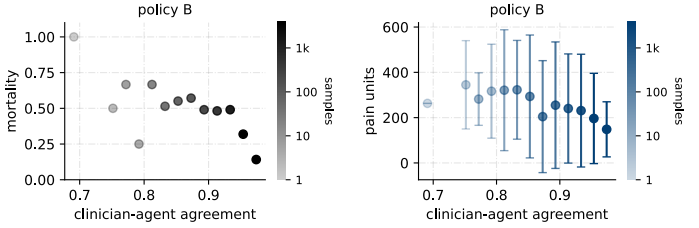


Fig. 6. Policy B displays an overall decreasing trend in the association between clinician-agent agreement, mortality, and cumulative pain. Points represent agreement-score bins, with color intensity indicating the number of cases per bin. For mortality (left), the vertical axis reports the empirical mortality rate. For cumulative pain (right), points denote the mean cumulative pain per bin, while error bars indicate the standard deviation.

This suggests that, while  $\pi_{\phi_A}$  and  $\pi_{\phi_B}$  generally behaved similarly to the clinician policy, they diverged from expected behavior in specific scenarios. The distinction was most evident in higher-complexity cases, which were less frequent in the patient population. By examining how clinician-agent agreement varied with the Elixhauser Comorbidity Index (ECI), we confirmed that the policies responded differently to clinical complexity:  $\pi_{\phi_A}$  tended to reinforce dosing patterns typical of patients with more comorbidities, whereas  $\pi_{\phi_B}$  deviated from these patterns (Fig. 7).

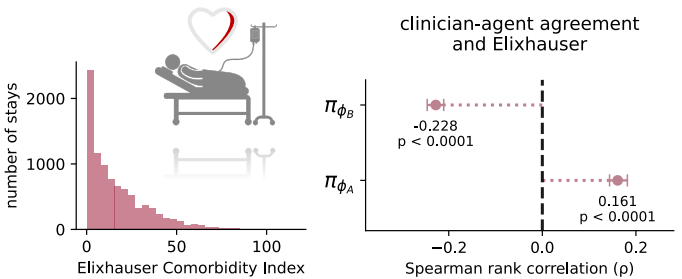


Fig. 7. Elixhauser Comorbidity Index (ECI) distribution (left) and correlations between clinician-agent agreement and ECI for test patients (right).

In particular, Fig. 8 shows that  $\pi_{\phi_A}$  responded to higher complexity with more aggressive, opioid-dominant strategies. Conversely,  $\pi_{\phi_B}$  moderated opioid dosing and relied primarily on more continuous propofol administration.

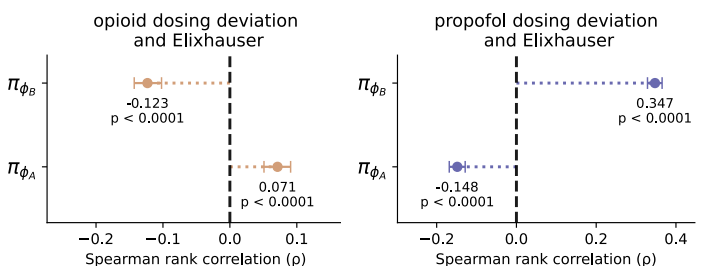


Fig. 8. Correlations between Elixhauser Comorbidity Index and signed deviation from the opioid and propofol doses administered by the clinicians.

As depicted in Fig. 9, we could find specific evidence of this behavior by studying individual high-complexity patients.

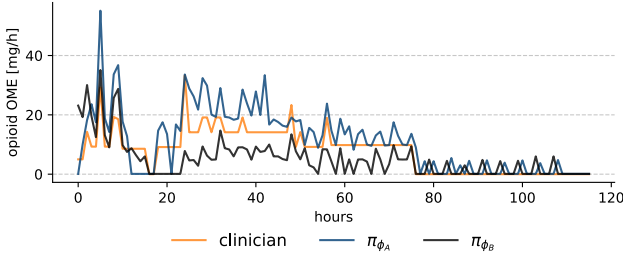


Fig. 9. Oral morphine-equivalent (OME) dosing for a test patient with an Elixhauser Comorbidity Index of 21. When comparing the clinician, policy A ( $\pi_{\phi_A}$ ) and policy B ( $\pi_{\phi_B}$ ), the latter is considerably more conservative.

Fig. 10 further illustrates that propofol use patterns were one of the key differences between the two policies. In fact, when stratifying the association between mortality and clinician-agent agreement by individual medications, propofol use can be identified as the primary driver for  $\pi_{\phi_B}$ 's association with lower mortality. This finding is consistent with prior adult ICU studies of opioid-propofol-based sedation and analgesia, which suggest that balanced regimens were associated with improved length of stay and mechanical ventilation outcomes when compared to opioid-dominant sedation [50]–[52].

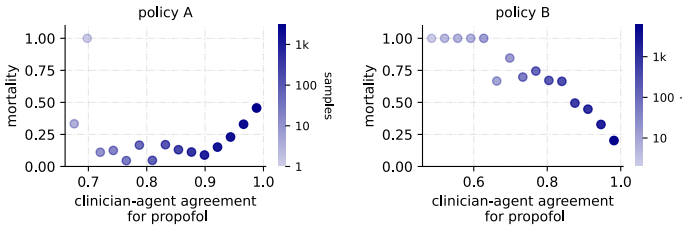


Fig. 10. Panels correspond to policy A (left) and policy B (right). Points denote propofol-dose agreement bins. Similarity to policy B is associated with lower empirical mortality, while the opposite is true for policy A.

## VI. CONCLUSION

Data-driven RL offers a promising framework for the support of complex clinical decision-making in the ICU. To fully realize its potential, though, it is essential to carefully consider all the challenges associated with goal specification, imperfect information, or lack of exploration.

In line with these principles, the present work focused on investigating the risks of optimizing a single short-term goal (pain reduction) in a safety-sensitive setting. We provide evidence that pain minimization without considering long-term outcomes leads to actions associated with increased mortality in the ICU up to 30 days after discharge. This highlights a potentially critical safety limitation in previous studies, which relied on short-term clinical signals such as mean arterial pressure. In contrast, we demonstrated that explicitly valuing both pain relief and patient survival enabled the learning of data-driven RL policies associated with lower patient mortality across a large dataset with diverse comorbidity profiles.

In obtaining these results, we extended prior research along three main dimensions. First, we modeled a richer and higher-dimensional action space, expanding from two continuous medication doses or 27 discrete options, to four continuous actions based on eight distinct drugs, including sedatives and analgesics. Second, we addressed partial observability by learning recurrent representations of the patient state, while strengthening offline learning with state-of-the-art regularization strategies. Third, we achieved a seven-fold increase in cohort size over prior studies (which analyzed at most 6,843 admissions) by leveraging records from 47,144 ICU stays. To the best of our knowledge, this represents the most data-comprehensive study on RL for sedation and analgesia.

These findings, however, should be interpreted as preliminary and observational; the reported effects are modest in magnitude, which is expected given the highly heterogeneous and noisy clinical data derived from real-world ICU practice. In addition, they reflect statistical associations rather than causal relationships. Addressing additional questions related to distributional shift and specification gaming will be essential to further assess the clinical significance of these results, particularly with respect to patient severity and treatment interactions. To improve the robustness, generalization, and safety of learned policies, future work will focus on incorporating causal modeling and strengthening evaluation through validation on multi-center cohorts.

## ACKNOWLEDGMENT

J.R. receives support from a Joan Oró research grant co-funded by Generalitat de Catalunya and the European Union (grant code: 2025 FI-1 00332). Previously, the research that led to these results was supported by a postgraduate fellowship awarded to J.R. by "la Caixa" Foundation (ID 100010434) (fellowship code: B005785).

## REFERENCES

- [1] P. N. Azzam and A. Alam, "Pain in the icu: a psychiatric perspective," *Journal of intensive care medicine*, vol. 28, no. 3, pp. 140–150, 2013.
- [2] J. A. Harvin and L. S. Kao, "Pain management in the surgical icu patient," *Current opinion in critical care*, vol. 26, no. 6, pp. 628–633, 2020.
- [3] J. P. Stevens, M. J. Wall, L. Novack, J. Marshall, D. J. Hsu, and M. D. Howell, "The critical care crisis of opioid overdoses in the united states," *Annals of the American Thoracic Society*, vol. 14, no. 12, pp. 1803–1809, 2017.
- [4] K. S. Lewis, J. K. Whipple, K. A. Michael, and E. J. Quebbeman, "Effect of analgesic treatment on the physiological consequences of acute pain," *American Journal of Health-System Pharmacy*, vol. 51, no. 12, pp. 1539–1554, 1994.
- [5] N. A. Desbiens, A. W. Wu, S. K. Broste, N. S. Wenger, A. F. Connors, J. Lynn, Y. Yasui, R. S. Phillips, and W. Fulkerson, "Pain and satisfaction with pain control in seriously ill hospitalized adults: findings from the support research investigations," *Critical care medicine*, vol. 24, no. 12, pp. 1953–1961, 1996.
- [6] A. K. Langerud, T. Rustøen, C. Brunborg, U. Kongsgaard, and A. Stubhaug, "Prevalence, location, and characteristics of chronic pain in intensive care survivors," *Pain Management Nursing*, vol. 19, no. 4, pp. 366–376, 2018.
- [7] S. G. Memtsoudis, R. Rasul, S. Suzuki, J. Poeran, T. Danninger, C. Wu, M. Mazumdar, and V. Vougioukas, "Does the impact of the type of anesthesia on outcomes differ by patient age and comorbidity burden?" *Regional Anesthesia & Pain Medicine*, vol. 39, no. 2, pp. 112–119, 2014.

[8] S. Alderson and S. McKechnie, "Unrecognised, undertreated, pain in icu—causes, effects, and how to do better," *Open Journal of Nursing*, vol. 3, no. 1, pp. 108–113, 2013.

[9] L. S. Simon, "Relieving pain in america: a blueprint for transforming prevention, care, education, and research," *Journal of pain & palliative care pharmacotherapy*, vol. 26, no. 2, pp. 197–198, 2012.

[10] D. J. Gaskin and P. Richard, "The economic costs of pain in the united states," *The journal of pain*, vol. 13, no. 8, pp. 715–724, 2012.

[11] S. Levine, A. Kumar, G. Tucker, and J. Fu, "Offline reinforcement learning: Tutorial, review, and perspectives on open problems," *arXiv preprint arXiv:2005.01643*, 2020.

[12] S. Liu, K. C. See, K. Y. Ngiam, L. A. Celi, X. Sun, and M. Feng, "Reinforcement learning for clinical decision support in critical care: comprehensive review," *Journal of medical Internet research*, vol. 22, no. 7, p. e18477, 2020.

[13] S. Nemat, M. M. Ghassemi, and G. D. Clifford, "Optimal medication dosing from suboptimal clinical examples: A deep reinforcement learning approach," in *2016 38th annual international conference of the IEEE engineering in medicine and biology society (EMBC)*. IEEE, 2016, pp. 2978–2981.

[14] A. Raghav, M. Komorowski, I. Ahmed, L. Celi, P. Szolovits, and M. Ghassemi, "Deep reinforcement learning for sepsis treatment," *arXiv preprint arXiv:1711.09602*, 2017.

[15] W.-H. Weng, M. Gao, Z. He, S. Yan, and P. Szolovits, "Representation and reinforcement learning for personalized glycemic control in septic patients," *arXiv preprint arXiv:1712.00654*, 2017.

[16] T. Li, Z. Wang, W. Lu, Q. Zhang, and D. Li, "Electronic health records based reinforcement learning for treatment optimizing," *Information Systems*, vol. 104, p. 101878, 2022.

[17] H. Zheng, J. Zhu, W. Xie, and J. Zhong, "Reinforcement learning assisted oxygen therapy for covid-19 patients under intensive care," *BMC medical informatics and decision making*, vol. 21, no. 1, p. 350, 2021.

[18] N. Prasad, L.-F. Cheng, C. Chivers, M. Draugelis, and B. E. Engelhardt, "A reinforcement learning approach to weaning of mechanical ventilation in intensive care units," *arXiv preprint arXiv:1704.06300*, 2017.

[19] C. Yu, J. Liu, and H. Zhao, "Inverse reinforcement learning for intelligent mechanical ventilation and sedative dosing in intensive care units," *BMC medical informatics and decision making*, vol. 19, no. 2, pp. 111–120, 2019.

[20] C. Yu, G. Ren, and Y. Dong, "Supervised-actor-critic reinforcement learning for intelligent mechanical ventilation and sedative dosing in intensive care units," *BMC medical informatics and decision making*, vol. 20, no. 3, pp. 1–8, 2020.

[21] D. Lopez-Martinez, P. Eschenfeldt, S. Ostvar, M. Ingram, C. Hur, and R. Picard, "Deep reinforcement learning for optimal critical care pain management with morphine using dueling double-deep q networks," in *2019 41st Annual International Conference of the IEEE Engineering in Medicine and Biology Society (EMBC)*. IEEE, 2019, pp. 3960–3963.

[22] N. Eghbali, T. Alhanai, and M. M. Ghassemi, "Patient-specific sedation management via deep reinforcement learning," *Frontiers in Digital Health*, vol. 3, p. 608893, 2021.

[23] ——, "Reinforcement learning approach to sedation and delirium management in the intensive care unit," in *2023 IEEE EMBS International Conference on Biomedical and Health Informatics (BHI)*, 2023, pp. 1–5.

[24] R. S. Sutton and A. G. Barto, *Reinforcement learning: An introduction*. MIT press, 2018.

[25] D. Silver, G. Lever, N. Heess, T. Degris, D. Wierstra, and M. Riedmiller, "Deterministic policy gradient algorithms," in *International conference on machine learning*. Pmlr, 2014, pp. 387–395.

[26] T. P. Lillicrap, J. J. Hunt, A. Pritzel, N. Heess, T. Erez, Y. Tassa, D. Silver, and D. Wierstra, "Continuous control with deep reinforcement learning," *arXiv preprint arXiv:1509.02971*, 2015.

[27] S. Fujimoto, D. Meger, and D. Precup, "Off-policy deep reinforcement learning without exploration," in *International conference on machine learning*. PMLR, 2019, pp. 2052–2062.

[28] S. Thrun and A. Schwartz, "Issues in using function approximation for reinforcement learning," in *Proceedings of the 1993 connectionist models summer school*. Psychology Press, 2014, pp. 255–263.

[29] H. Van Hasselt, A. Guez, and D. Silver, "Deep reinforcement learning with double q-learning," in *Proceedings of the AAAI conference on artificial intelligence*, vol. 30, no. 1, 2016.

[30] A. Kumar, J. Fu, M. Soh, G. Tucker, and S. Levine, "Stabilizing off-policy q-learning via bootstrapping error reduction," *Advances in neural information processing systems*, vol. 32, 2019.

[31] A. Kumar, A. Zhou, G. Tucker, and S. Levine, "Conservative q-learning for offline reinforcement learning," *Advances in Neural Information Processing Systems*, vol. 33, pp. 1179–1191, 2020.

[32] L. P. Kaelbling, M. L. Littman, and A. R. Cassandra, "Planning and acting in partially observable stochastic domains," *Artificial intelligence*, vol. 101, no. 1-2, pp. 99–134, 1998.

[33] A. E. Johnson, L. Bulgarelli, L. Shen, A. Gayles, A. Shammout, S. Horng, T. J. Pollard, S. Hao, B. Moody, B. Gow *et al.*, "Mimic-iv, a freely accessible electronic health record dataset," *Scientific data*, vol. 10, no. 1, p. 1, 2023.

[34] S. Nielsen, L. Degenhardt, B. Hoban, and N. Gisev, "A synthesis of oral morphine equivalents (ome) for opioid utilisation studies," *Pharmacoepidemiology and drug safety*, vol. 25, no. 6, pp. 733–737, 2016.

[35] K. McKeage and C. M. Perry, "Propofol: a review of its use in intensive care sedation of adults," *CNS drugs*, vol. 17, no. 4, pp. 235–272, 2003.

[36] W. B. Cammarano, J.-F. Pittet, S. Weitz, R. M. Schlobohm, and J. D. Marks, "Acute withdrawal syndrome related to the administration of analgesic and sedative medications in adult intensive care unit patients," *Critical care medicine*, vol. 26, no. 4, pp. 676–684, 1998.

[37] J. Barr, K. Zomorodi, E. J. Bertaccini, S. L. Shafer, and E. Geller, "A double-blind, randomized comparison of iv lorazepam versus midazolam for sedation of icu patients via a pharmacologic model," *The Journal of the American Society of Anesthesiologists*, vol. 95, no. 2, pp. 286–298, 2001.

[38] N. Bhana, K. L. Goa, and K. J. McClellan, "Dexmedetomidine," *Drugs*, vol. 59, no. 2, pp. 263–268, 2000.

[39] M. Gupta, B. Gallamoza, N. Cutrona, P. Dhakal, R. Poulain, and R. Beheshti, "An extensive data processing pipeline for mimic-iv," in *Machine learning for health*. PMLR, 2022, pp. 311–325.

[40] C. Hug, "Detecting hazardous intensive care patient episodes using real-time mortality models," Ph.D. dissertation, Massachusetts Institute of Technology, 2009.

[41] I. R. White, P. Royston, and A. M. Wood, "Multiple imputation using chained equations: issues and guidance for practice," *Statistics in medicine*, vol. 30, no. 4, pp. 377–399, 2011.

[42] A. Natekin and A. Knoll, "Gradient boosting machines, a tutorial," *Frontiers in neurorobotics*, vol. 7, p. 21, 2013.

[43] C. Kingsford and S. L. Salzberg, "What are decision trees?" *Nature biotechnology*, vol. 26, no. 9, pp. 1011–1013, 2008.

[44] T. Chen and C. Guestrin, "Xgboost: A scalable tree boosting system," in *Proceedings of the 22nd ACM SIGKDD international conference on knowledge discovery and data mining*, 2016, pp. 785–794.

[45] J. Liu, J. Wu, S. Liu, M. Li, K. Hu, and K. Li, "Predicting mortality of patients with acute kidney injury in the icu using xgboost model," *Plos one*, vol. 16, no. 2, p. e0246306, 2021.

[46] K. Cho, B. Van Merriënboer, D. Bahdanau, and Y. Bengio, "On the properties of neural machine translation: Encoder-decoder approaches," *arXiv preprint arXiv:1409.1259*, 2014.

[47] N. Heess, J. J. Hunt, T. P. Lillicrap, and D. Silver, "Memory-based control with recurrent neural networks," *arXiv preprint arXiv:1512.04455*, 2015.

[48] S. Fujimoto, H. Hoof, and D. Meger, "Addressing function approximation error in actor-critic methods," in *International conference on machine learning*. PMLR, 2018, pp. 1587–1596.

[49] S. Fujimoto and S. S. Gu, "A minimalist approach to offline reinforcement learning," *Advances in neural information processing systems*, vol. 34, pp. 20132–20145, 2021.

[50] B. Muellejans, T. Matthey, J. Scholpp, and M. Schill, "Sedation in the intensive care unit with remifentanil/propofol versus midazolam/fentanyl: a randomised, open-label, pharmacoeconomic trial," *Critical Care*, vol. 10, no. 3, p. R91, 2006.

[51] F. W. Rozendaal, P. E. Spronk, F. F. Snellen, A. Schoen, A. R. van Zanten, N. A. Foudraire, P. G. Mulder, J. Bakker, and other UltiSAFE investigators, "Remifentanil-propofol analgo-sedation shortens duration of ventilation and length of icu stay compared to a conventional regimen: a centre randomised, cross-over, open-label study in the netherlands," *Intensive care medicine*, vol. 35, no. 2, pp. 291–298, 2009.

[52] A. C. Faust, P. Rajan, L. A. Sheperd, C. A. Alvarez, P. McCorstin, and R. L. Doebele, "Impact of an analgesia-based sedation protocol on mechanically ventilated patients in a medical intensive care unit," *Anesthesia & Analgesia*, vol. 123, no. 4, pp. 903–909, 2016.